Available online at www.sciencedirect.com

SciVerse ScienceDirect

Ceramics International 39 (2013) 1951–1956

CERAMICS INTERNATIONAL

www.elsevier.com/locate/ceramint

Effect of Yb^{3+} and Tm^{3+} concentrations on blue and NIR upconversion luminescence in Yb^{3+}, Tm^{3+} co-doped $CaMoO_4$

Jun Ho Chung[a], Jeong Ho Ryu[b,*], Sang Yeop Lee[a], Suk Hyun Kang[a], Kwang Bo Shim[a]

[a]*Department of Materials Science and Engineering, Hanyang University, 17 Haengdang-dong Seongdong-gu, Seoul 133-791, South Korea*
[b]*Department of Materials Science and Engineering, Korea National University of Transportation, 50 Daehak-ro, Chungju-si, Chungbuk 380-702, South Korea*

Received 9 August 2012; accepted 15 August 2012
Available online 23 August 2012

Abstract

Polycrystalline Tm^{3+}/Yb^{3+} co-doped $CaMoO_4$ UC phosphors were successfully synthesized by a complex citrate-gel method and their upconversion (UC) luminescence was investigated. Under excitation at 980 nm, Tm^{3+}/Yb^{3+} co-doped $CaMoO_4$ showed bright blue emission near 475 nm generated by the $^1G_4 \rightarrow {}^3H_6$ transition and strong NIR UC emission around 796 nm generated by the $^3H_4 \rightarrow {}^3H_6$ transition, with weak red emission near 650 nm due to the $^3F_2 \rightarrow {}^3H_6$ transition. The optimum doping concentrations of Tm^{3+} and Yb^{3+} for the highest UC luminescence were investigated, and the related UC mechanism of Tm^{3+}/Yb^{3+} co-doped $CaMoO_4$ depending on pump power was studied in detail.

Keywords: Tm^{3+}/Yb^{3+} co-doped $CaMoO_4$; Upconversion (UC) luminescence; Upconversion mechanism

1. Introduction

In recent years, rare-earth (RE) doped luminescent materials have received extensive attention for their potential applications such as phosphors [1,2], solar cells [3], flat-panel displays [4,5], scintillators [6], and solid state lasers [7]. Among them, UC luminescence from the near-infrared (NIR) region to the visible region, which can convert from low energy to higher energy radiation via multiple absorption or energy transfer, has been actively studied [8,9] due to their applications for biology and biomedicine such as fluorescent labels and biological probes for investigation or sensitive detection of biomolecules [10]. Trivalent lanthanide ions such as Er^{3+}, Tm^{3+} and Ho^{3+} are commonly used as activator ions for UC luminescence due to their abundant energy levels for radiative transition. In particular, Tm^{3+} is an excellent candidate for a UC luminescent center because of its unique properties such as blue emission around 480 nm and NIR emission near 800 nm [11,12]. However, Tm^{3+} has a very low absorption cross section around 980 nm. Therefore, a sensitizer ion is required to achieve upper level population through energy transfer. Yb^{3+} is usually chosen as the sensitizer in UC materials in order to facilitate efficient energy transfer from the sensitizer to Tm^{3+} ion because Yb^{3+} has a large absorption cross-section near 980 nm [13].

For higher efficiency UC luminescence, stable upconverting materials with low excitation thresholds are very important. Metal oxide materials are usually very stable chemically, mechanically and thermally, and could therefore be promising host matrices for light upconverting applications. However, to date, most research on RE-doped UC has focused on halides [14], glasses [15] and simple oxides [16,17].

One of the metal molybdates with a scheelite structure, $CaMoO_4$, is an excellent candidate for host matrices because it has high density (4.25 g/cm^3) and more stable physical and chemical properties compared to other oxide materials [18,19]. In addition, the Mo^{6+} ions in $CaMoO_4$ matrices have strong polarization induced by large electric charges and a small radius, which consequently decreases symmetry and enhances Stark energy splitting in the crystal field [20]. We already reported blue and NIR UC luminescence in $Li^+/Tm^{3+}/Yb^{3+}$ co-doped $CaMoO_4$ [21]. However, effect of Tm^{3+} and Yb^{3+} concentrations on UC

---

*Corresponding author. Tel.: +82 43 841 5384; fax: +82 43 841 5380.
E-mail address: jhryu@ut.ac.kr (J.H. Ryu).

0272-8842/$ - see front matter © 2012 Elsevier Ltd and Techna Group S.r.l. All rights reserved.
http://dx.doi.org/10.1016/j.ceramint.2012.08.045

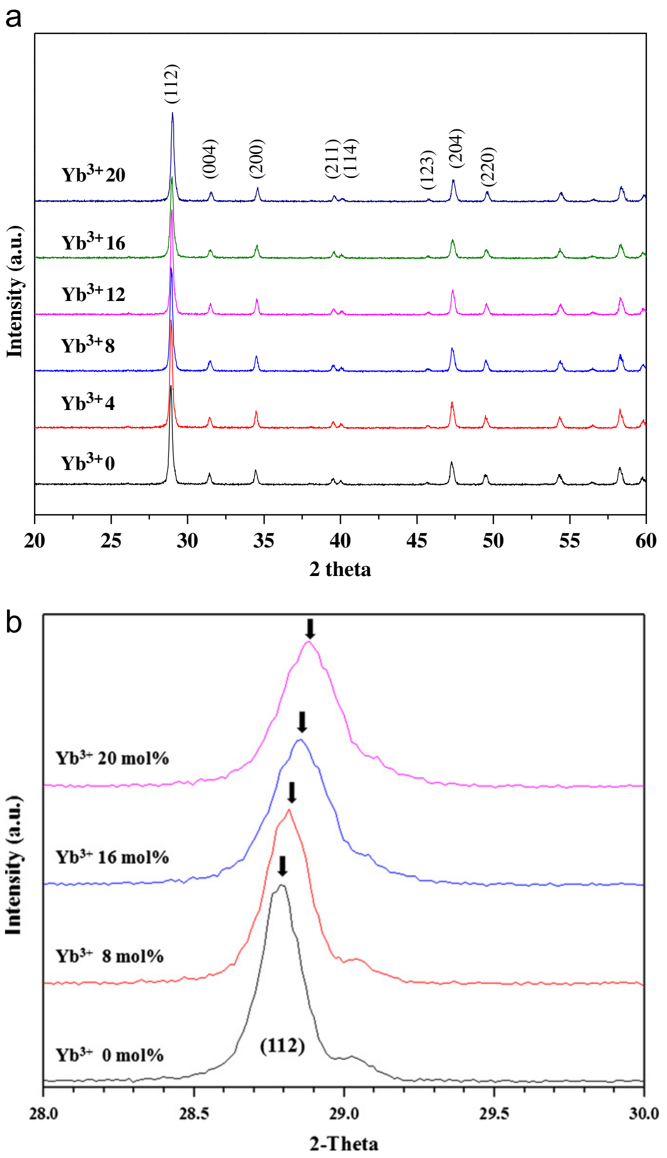

Fig. 1. (a) X-ray diffraction patterns of Tm^{3+}/Yb^{3+} co-doped $CaMoO_4$ upconversion phosphors with Yb^{3+} concentrations varied from 0 to 20 mol% calcined at 600 °C for 3 h. (b) Enlarged XRD patterns near $2\theta=29°$ for the (112) peak.

luminescence from Tm^{3+}/Yb^{3+} co-doped $CaMoO_4$ has not been studied yet. Consequently, the development of a Tm^{3+}/Yb^{3+} co-doped $CaMoO_4$ system and the establishment of a mechanism relating the efficiency of NIR to visible UC luminescence are expected to have a great impact on broadening potential application fields.

In the present work, we synthesized the strong blue emitting oxide UC phosphors through Tm^{3+}/Yb^{3+} co-doping into $CaMoO_4$ matrix by the citrate-gel method and investigated effect of Tm^{3+}/Yb^{3+} concentrations on UC luminescence from Tm^{3+}/Yb^{3+} co-doped $CaMoO_4$. The properties of structure and photoluminescence under excitation of 980 nm were investigated. Moreover, the effects of co-doped Tm^{3+} and Yb^{3+} ions in $CaMoO_4$ matrix on the intensity of UV emission and luminescent mechanism are studied in detail.

2. Experimental procedure

2.1. Starting materials

Tm^{3+}/Yb^{3+} co-doped $CaMoO_4$ were prepared by a complex citrate-gel method with microwave assistance [21]. The starting materials were calcium nitrates ($Ca(NO_3)_2\cdot 4H_2O$, purity 99.99%, Junsei Chemical Co. Ltd., Japan), ammonium molybdate ($(NH_4)_6\ Mo_7O_{24}\cdot 4H_2O$, 99.99%, Junsei Chemical Co., Ltd., Japan), ytterbium chloride hydrate ($YbCl_3\cdot xH_2O$ ($x=6$), 99.99%, Alfa Aesar) and thulium nitrate hydrate ($Tm(NO_3)_3\cdot xH_2O$ ($x=5$), 99.99%, Alfa Aesar), which were dissolved in DI water with citric acid (metal cation:citric acid = 1:2).

2.2. Preparation and synthesis of Tm^{3+}/Yb^{3+} co-doped $CaMoO_4$

The molar ratios of the metal cations were as follows: $(1-x-y)\ Ca^{2+}+xTm^{3+}+yYb^{3+}+Mo^{6+}$; $x=0$, 0.02, 0.05, 0.1, 1.5, 2 and 3; $y=0$, 0.04, 0.08, 0.12, 0.16 and 0.20. The solution was kept at 100 °C for 10 min under constant stirring until it became viscous. The solution was then microwave-treated for a 30-min period with an on-time duration of 2 min and an off-time duration of 1 min in ambient atmosphere until a gel was formed. The gel was heated in an oven at 250 °C for 24 h in order to remove organic substances and evaporating moisture, until an yellow dried powder was obtained. The powder was calcined at 600 °C for 3 h at ambient atmosphere.

2.3. Characterization

Phase analysis was performed using an X-ray diffractometer (XRD, Rigaku D/MAX2C, Japan, Cu-α ($\lambda=1.5046$ Å)). The UC luminescence spectra and power-dependent properties were evaluated using photoluminescence spectroscopy (PerkinElmer, LS55, USA) at room temperature with a range of wavelengths from 400 nm to900 nm under excitation at 980 nm, and the pump power for irradiation was varied from 20 mW to 110 mW (SPEX, 1404p, France).

3. Results and discussion

3.1. Structural and optical analysis of Tm^{3+}/Yb^{3+} co-doped $CaMoO_4$

Fig. 1(a) shows the XRD patterns of Tm^{3+}/Yb^{3+} co-doped $CaMoO_4$ with various Yb^{3+} ion concentrations calcined at 600 °C for 3 h. We did not observe any impurities or secondary phases, implying that the charge difference induced by trivalent ions (Tm^{3+},Yb^{3+}) doped into the site of bivalent host ions (Ca^{2+}) did not affect the structural properties [22]. However, with increasing Yb^{3+} concentrations, the diffraction peaks were shifted to a higher 2θ angle, illustrating substitution of Yb^{3+} ions into Ca^{2+} ion sites and

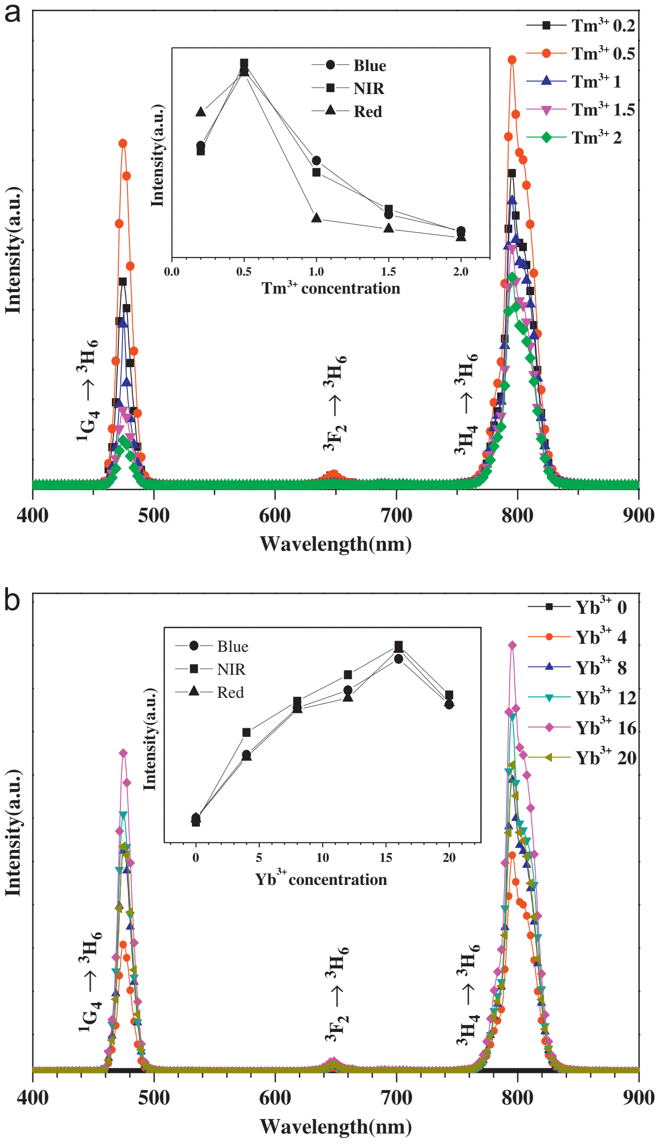

Fig. 2. Photoluminescence (PL) spectra of $CaMoO_4$ UC phosphors with (a) Tm^{3+} concentrations ranging from 0.2 to 2 mol% and (b) Yb^{3+} concentrations ranging from 0 to 20 mol%. The inset represents the variation in UC luminescence emission intensity with increasing (a) Tm^{3+} and (b) Yb^{3+} concentrations. (For interpretation of the references to color in this figure legend, the reader is referred to the web version of this article.)

the resultant shrinkage of lattice constants (Fig. 1b). Moreover, broadening of the diffraction peaks at (112) at increased Yb^{3+} concentrations implied that a high doping concentration of Yb^{3+} ions would lead to a decrease in crystallinity due to lattice shrinkage of the $CaMoO_4$ matrix.

Fig. 2 presents that (a) effect of Tm^{3+} concentration on the intensity of UC luminescence at fixed Yb^{3+} concentrations (8 mol%) and (b) effect of Yb^{3+} concentration in Tm^{3+}/Yb^{3+} co-doped $CaMoO_4$ at a fixed Tm^{3+} concentration (0.5 mol%) within the range of 400–900 nm. As shown in Fig. 2(a), at a fixed Yb^{3+} concentration (8 mol%), the intensities of all emission regions were increased with increased Tm^{3+} concentration up to 0.5 mol%, and then decreased at concentrations over 0.5 mol%. Moreover, shown in Fig. 2(b), with increasing Yb^{3+} concentrations up to 16 mol%, the intensities of all emission regions increased, while emission intensities declined at concentrations over 16 mol% due to a quenching effect [23]. This concentration quenching effect could be explained by the energy transfer between the nearest dopant (activator→activator or sensitizer→activator) ions. As dopant ion concentrations are increased, the distance between dopant ions shrinks, allowing non-radiative energy transfer such as exchange or multipole–multipole interactions. Based on our results, we concluded that the optimum Tm^{3+}/Yb^{3+} doping concentrations were 0.5/16 mol% (summarized in the inset of Fig. 2(a) and (b)). The UC emissions in Tm^{3+}/Yb^{3+} co-doped $CaMoO_4$ were dominated by strong blue emission and NIR emission while red emission was weaker than blue and NIR. The UC luminescent spectra of Tm^{3+}/Yb^{3+} co-doped $CaMoO_4$ consisted of the following three regions: (1) NIR emission at 796 nm, which could be attributed to the $^3H_4 \rightarrow {}^3H_6$ transition; (2) strong blue emissions near 475 nm assigned to the $^1G_4 \rightarrow {}^3H_6$ transition; and (3) relatively weak red emission attributed to the $^3F_2 \rightarrow {}^3H_6$ transition around 650 nm, caused by intra 4f–4f transitions of Tm^{3+} ions [24].

Fig. 3 shows the commission internationale de l'Eclairage (CIE) chromaticity diagrams of 0.5% Tm^{3+}/16% Yb^{3+} co-doped $CaMoO_4$ under laser excitation at 980 nm (fixed at 100 mW). The Tm^{3+}/Yb^{3+} co-doped $CaMoO_4$ (0.5/16 mol%) sample exhibits strong blue emission visible to the naked eye under excitation at 980 nm (inset of Fig. 3). The corresponding chromaticity coordinates are $x=0.116$ and $y=0.085$, which are imbedded in the blue luminescent region of Fig. 3. Based on our results we therefore suggest that Tm^{3+}/Yb^{3+} co-doped $CaMoO_4$ is an excellent candidate for blue and NIR UC phosphors.

The blue, NIR and red intensities of $CaMoO_4$ co-doped with Tm^{3+}/Yb^{3+} to 0.5/16 mol% in a logarithmic diagram as a function of pump power are plotted in Fig. 4. In the UC process, the intensity of emission is proportional to the nth value of the irradiation pump power [25]:

$$I \propto P^n$$

where n is the number of pumping photons required to excite the emitting state, I is the luminescent intensity and P is the laser pumping power. The calculated results indicated that the slopes of the n values were 2.73, 1.75 and 1.59 for blue emission, NIR emission and red emission, respectively. The n value for blue emission ($^1G_4 \rightarrow {}^3H_6$) was over 2 and close to 3, while that for NIR ($^3H_4 \rightarrow {}^3H_6$) and red emission ($^3F_2 \rightarrow {}^3H_6$) was less than 2. This result implies that the UC mechanism corresponding to blue emission can be explained by a three-photon process, while NIR and red emissions can be induced by a two-photon process [25].

3.2. *Possible upconversion mechanism of Tm^{3+}/Yb^{3+} co-doped $CaMoO_4$*

Based on the above results, UC mechanisms of the blue, NIR and red emissions of Tm^{3+}/Yb^{3+} co-doped $CaMoO_4$ are schematically illustrated in Fig. 5. Under excitation at

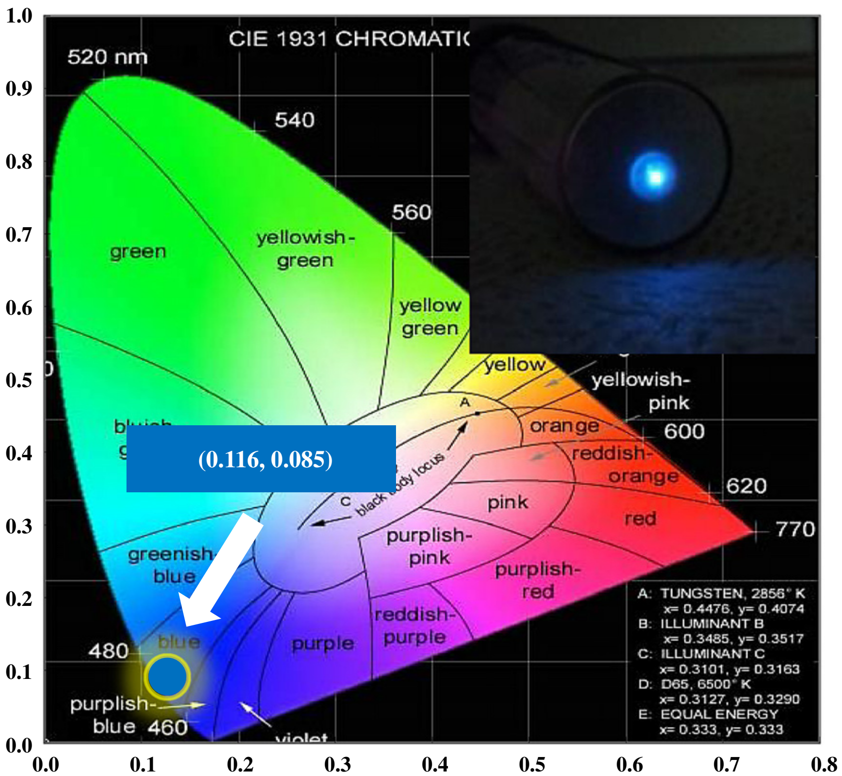

Fig. 3. The Commission Internationale de l'Éclairage (CIE) chromaticity diagrams of 0.5% Tm^{3+}/16% Yb^{3+} co-doped $CaMoO_4$ under excitation at 980 nm. The inset photograph shows strong blue emission for the Tm^{3+}/Yb^{3+} (0.5/16 mol%) co-doped $CaMoO_4$ sample visible to the naked eye under 980 nm excitation. (For interpretation of the references to color in this figure legend, the reader is referred to the web version of this article.)

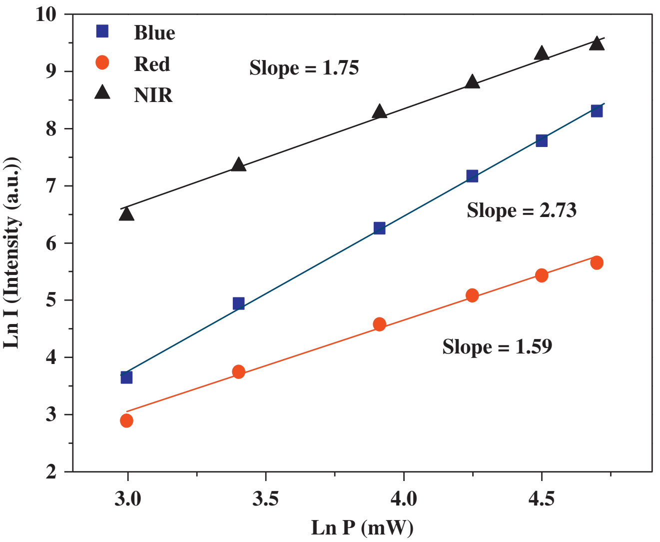

Fig. 4. Pump power dependence of upconversion emission on the working current from 20 to 110 mW at blue, NIR and red UC emission centers with fixed dopant concentrations of 0.5 mol% Tm^{3+} and 16 mol% Yb^{3+}. (For interpretation of the references to color in this figure legend, the reader is referred to the web version of this article.)

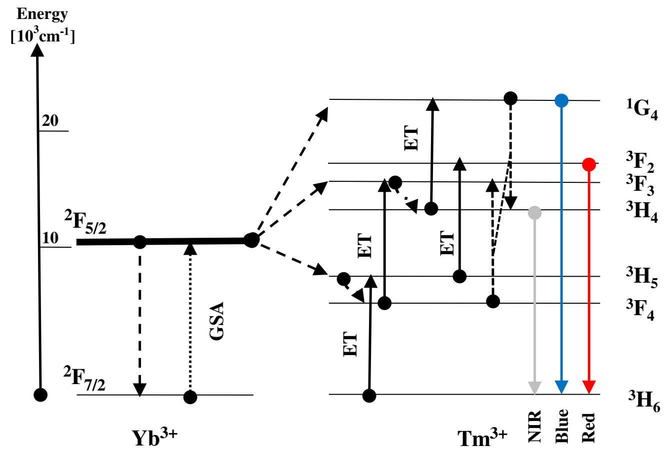

Fig. 5. Energy level diagrams of Tm^{3+} and Yb^{3+} co-doped $CaMoO_4$ upconversion phosphors and possible UC mechanisms under excitation at 980 nm.

980 nm, non-resonant energy transfer occurs from the $^2F_{5/2}$ state in the Yb^{3+} to the $^3H_5$ level in the Tm^{3+} and/or ground state absorption (GSA) process by a $^3H_6 \rightarrow {}^3H_5$ transition. The subsequent $^3H_5 \rightarrow {}^3F_4$ transition can be generated by non-radiative relaxation. The $^3F_3$ state can then be excited from the $^3F_4$ state through excited state absorption (ESA) or energy transfer upconversion (ETU) generating the metastable $^3H_4$ state from a non-radiative transition, which plays an important role in the generation of blue and NIR emissions [24]. For blue emission, the $^3H_4$ state can be further excited to the $^1G_4$ state through ESA or ETU. Finally, the $^1G_4 \rightarrow {}^3H_6$ transition generates the

blue emission center [24,26]. For NIR emission, the metastable $^3H_4$ state that is not excited to the high energy state in Tm^{3+}, such as the $^1G_4$ state, generates the NIR emission by radiative transition of $^3H_4 \rightarrow {}^3H_6$. The red emission is assigned to the $^3F_2 \rightarrow {}^3H_6$ transition [24,26]. The $^3F_2$ state can be populated only by the $^3H_5 \rightarrow {}^3F_2$ transition by ESA and ETU processes. According to the energy gap law, the nonradiative transition of $^3H_5 \rightarrow {}^3F_4$ dominates rather than the $^3H_5 \rightarrow {}^3F_2$ transition because the energy gap between the $^3H_5$ and $^3F_4$ states is so small [26]. Therefore, the $^3F_2$ state cannot be populated well, underlying the weak red emission. Moreover, the intensity of the NIR emission is higher than that of the blue emission. This might be due to the increased population of the $^3H_4$ state [27]. The energy gap between $^1G_4$ and $^3H_4$ is smaller than that between $^3F_4$ and $^3F_2$ (740 cm^{-1}) [28]. Therefore, through the CR process, the energy transition of $^1G_4 \rightarrow {}^3H_4$ can easily populate the $^3F_3$ state instead of the $^3F_2$ state. Moreover, the $^3F_3$ state can easily relax to the $^3H_4$ state because the energy gap between $^3F_3$ and $^3H_4$ is so small, which can increase the population of the $^3H_4$ state and the radiative transition of $^3H_4 \rightarrow {}^3H_6$.

4. Conclusion

We synthesized and investigated UC luminescence of Tm^{3+}/Yb^{3+} co-doped $CaMoO_4$. The Tm^{3+}/Yb^{3+} co-doped $CaMoO_4$ phosphor has strong blue and NIR luminescent centers at 475 nm ($^1G_4 \rightarrow {}^3H_6$) and 796 nm ($^3H_4 \rightarrow {}^3H_6$), while it has a very weak red emission center around 650 nm ($^3F_2 \rightarrow {}^3H_6$) under 980 nm excitation. The optimum doping concentrations of Tm^{3+} and Yb^{3+} for the highest intensities of UC luminescence in the $CaMoO_4$ system are 0.5 mol% of Tm^{3+} and 16 mol% of Yb^{3+}. Power-dependent luminescent properties show that a three photon process is responsible for blue emission, while NIR and red emissions are dominated by a two-photon process. In particular, the intensity of NIR emission is higher than that of blue emission, which results from an easily populated $^3H_4$ state because the energy gap between $^1G_4$ and $^3H_4$ is smaller than that between $^3F_4$ and $^3F_2$. Based on our results and analysis, we conclude that Tm^{3+}/Yb^{3+} co-doped $CaMoO_4$ is an excellent candidate for blue and NIR UC phosphors.

Acknowledgment

The research was supported by a grant from the Academic Research Program of Korea National University of Transportation in 2012.

References

[1] P. Li, Q. Peng, Y. Li, Dual-mode luminescent colloidal spheres from monodisperse rare-earth fluoride nanocrystals, Advanced Materials 21 (2009) 1945–1948.

[2] L. Wang, R. Yan, Z. Huo, L. Wang, J. Zeng, J. Bao, X. Wang, Q. Peng, Y. Li, Fluorescence resonant energy transfer biosensor based on upconversion-luminescent nanoparticles, Angewandte Chemie—International Edition 44 (2005) 6054–6057.

[3] A. Shalav, B.S. Richards, M.A. Green, Luminescent layers for enhanced silicon solar cell performance: up-conversion, Solar Energy Materials and Solar Cells 91 (2007) 829–842.

[4] E. Downing, L. Hesselink, J. Ralston, R. Macfarlane, A three-color, solid-state, three-dimensional display, Science 273 (1996) 1185–1189.

[5] G.S. Maciel, A. Biswas, R. Kapoor, P.N. Prasad, Blue cooperative upconversion in Yb^{3+}-doped multicomponent sol–gel-processed silica glass for three-dimensional display, Applied Physics Letters 76 (2000) 1978–1980.

[6] G. Panayiotakis, D. Cavouras, I. Kandarakis, C. Nomicos, A study of X-ray luminescence and spectral compatibility of europium-activated yttrium-vanadate (YVO_4:Eu) screens for medical imaging applications, Applied Physics A 62 (1996) 483–486.

[7] F. Heine, E. Heumann, T. Danger, T. Schweizer, G. Huber, B. Chai, Green up-conversion continous-wave Er^{3+}:$LiYF_4$ laser at room-temperature, Applied Physics Letters 65 (1994) 383–384.

[8] F. Vetrone, V. Mahalingam, J.A. Capobianco, Near-infrared-to-blue upconversion in colloidal $BaYF_5$:Tm^{3+},Yb^{3+} nanocrystals, Chemistry of Materials 21 (2009) 1847–1851.

[9] C. Cao, W. Qin, J. Zhang, Y. Wang, G. Wang, G. Wei, P. Zhu, L. Wang, L. Jin, Up-conversion white light of $Tm^{3+}/Er^{3+}/Yb^{3+}$ tri-doped CaF_2 phosphors, Optics Communications 281 (2008) 1716–1719.

[10] P. Zhang, W. Steelant, M. Kumar, M. Scholfield, Versatile photosensitizers for photodynamic therapy at infrared excitation, Journal of the American Chemical Society 129 (2007) 4526–4527.

[11] J.F. Suyver, J. Grimin, M.K. van Veen, D. Biner, K.W. Kramer, H.U. Gudel, Upconversion spectroscopy and properties of $NaYF_4$ doped with Er^{3+}, Tm^{3+} and/or Yb^3, Journal of Luminescence 117 (2006) 1–12.

[12] Q.Y. Zhang, T. Li, Z.H. Jiang, X.H. Ji, B. Buddhudu, 980 nm Laser-diode-excited intense blue upconversion in Tm^{3+}/Yb^{3+}-codoped gallate–bismuth–lead glasses, Applied Physics Letters 87 (2005) 171911-1–3.

[13] V.P. Gapontsev, S.M. Matitsin, A.A. Isineev, V.B. Kravcheko, Erbium glass lasers and their applications, Optics and Laser Technology 14 (1982) 189–196.

[14] J.C. Boyer, F. Vetrone, L.A. Cupconversioncia, J.A. Capobianco, Synthesis of colloidal upconverting $NaYF_4$ nanocrystals doped with Er^{3+},Yb^{3+} and Tm^{3+},Yb^{3+} via thermal decomposition of lanthanide trifluoroacetate precursors, Journal of the American Chemical Society 128 (2006) 7444–7445.

[15] Y.H. Wang, J. Ohwaki, New transparent vitroceramics codoped with Er^{3+} and Yb^{3+} for efficient frequency up-conversion, Applied Physics Letters 63 (1993) 3268–3270.

[16] A.M. Pires, O.A. Serra, S. Heer, H.U. Güdel, Low-temperature upconversion spectroscopy of nanosized Y_2O_3:Er,Yb phosphor, Journal of Applied Physics 98 (2005) 063529-1–7.

[17] A. Patra, C.S. Friend, R. Kapoor, P.N. Prasad, Upconversion in Er^{3+}:ZrO_2 nanocrystals, Journal of Physical Chemistry B 106 (2002) 1909–1912.

[18] A. Phuruangrat, T. Thongtem, S. Thongtem, Preparation, characterization and photoluminescence of nanocrystalline calcium molybdate, Journal of Alloys and Compounds 481 (2009) 568–572.

[19] T. Thongtem, A. Phuruangrat, S. Thongtem, Sonochemical synthesis of $MMoO_4$ (M = Ca, Sr and Ba) nanocrystals, Journal of Ceramic Processing Research 9 (2008) 189–191.

[20] L.H.C. Andrade, M.S. Li, Y. Guyot, A. Brenier, G. Boulon, Optical multi-sites of Nd^{3+}-doped $CaMoO_4$ induced by Nb^{5+} charge compensator, Journal of Physics: Condensed Matter 18 (2006) 7883–7892.

[21] J.H. Chung, J.H. Ryu, J.W. Eun, J.H. Lee, S.Y. Lee, T.H. Heo, B.G. Choi, K.B. Shim, Green upconversion luminescence from poly-

crystalline Yb^{3+}, Er^{3+} Co-doped $CaMoO_4$, Journal of Alloys and Compounds 552 (2012) 30–34.

[22] J. Liu, H. lian, C. Shi, Improved optical photoluminescence by charge compensation in the phosphor system $CaMoO_4$:Eu^{3+}, Optical Materials 29 (2007) 1591–1594.

[23] D. Yang, C. Li, G. Li, M. Shang, X. Kang, J. Lin, Colloidal synthesis and remarkable enhancement of the upconversion luminescence of $BaGdF_5$:Yb^{3+}/Er^{3+} nanoparticles by active-shell modification, Journal of Materials Chemistry 21 (2011) 5923–5927.

[24] J.J. Li, L.W. Yang, Y.Y. Zhang, J.X. Zhong, C.Q. Sun, P.K. Chu, Pump-power tunable white upconversion emission in lanthanide-doped hexagonal $NaYF_4$ nanorods, Optical Materials 33 (2011) 882–887.

[25] I. Etchart, I. Hernandez, A. Huignard, M. Berard, M. Laroche, W.P. Gillin, R.J. Curry, A.K. Cheetham, Oxide phosphors for light upconversion; Yb^{3+} and Tm^{3+} co-doped Y_2BaZnO_5, Journal of Applied Physics 109 (2011) 063104-1–7.

[26] J.H. Chung, S.Y. Lee, K.B. Shim, S.Y. Kweon, S.C. Ur, J.H. Ryu, Blue upconversion luminescence of $CaMoO_4$:Li^{+}/Yb^{3+}/Tm^{3+} phosphors prepared by complex citrate method, Applied Physics A 108 (2012) 369–373.

[27] F. Wang, X.G. Liu, Upconversion multicolor fine-tuning: visible to near-infrared emission from lanthanide-doped $NaYF_4$ nanoparticles, Journal of the American Chemical Society 130 (2008) 5642–5643.

[28] K. Mishra, N.K. Girl, S.B. Rai, Preparation and characterization of upconversion luminescent Tm^{3+}/Yb^{3+} co-doped Y_2O_3 nanophosphor, Applied Physics B—Laser and Optics 103 (2011) 863–875.